



ELSEVIER

Available online at www.sciencedirect.com

SCIENCE @ DIRECT®

Nuclear Instruments and Methods in Physics Research A 526 (2004) 206–214

NUCLEAR
INSTRUMENTS
& METHODS
IN PHYSICS
RESEARCH
Section A

www.elsevier.com/locate/nima

A detector of bunch time structure for cw heavy-ion beams

N.E. Vinogradov*, P.N. Ostroumov, R.C. Pardo, S.I. Sharamentov, G.P. Zinkann

Argonne National Laboratory, Physics Division, 9700 S. Cass Ave, Argonne, IL, USA

Received 14 November 2003; received in revised form 9 February 2004; accepted 12 February 2004

Abstract

The manuscript describes the design, commissioning and performance of a new device for the measurement of bunch time structure of heavy-ion beams. The Bunch Length Detector (BLD) has been developed, constructed and installed at the Argonne Tandem Linear Accelerating System, a superconducting linac. The BLD is a wire scanning detector based on the analysis of secondary electrons produced by the primary beam hitting a target wire. The device provides measuring of bunch phase spectrum for ion beams in a wide range of energies, intensities and species in cw mode with up to 20 ps resolution.

© 2004 Elsevier B.V. All rights reserved.

PACS: 29.27.Fh; 79.20.Hx; 42.79.Fm

Keywords: Bunch shape; Secondary electrons; RF deflector

1. Introduction

Measurements of the longitudinal distribution of charge in a bunch and the longitudinal emittance are among the most important tools for a beam dynamics study or an accelerator tune. The main requirements of a bunch shape detector are: high time resolution, low beam distortion and a wide range of measurements in primary beam characteristics [1]. The principle of operation, various applications and some historical review of the Bunch Length Detectors (BLDs) were reported elsewhere [1,2]. All previously developed BLDs operate in pulsed mode and were assigned for the measurements in low duty cycle accelerators.

The BLD presented here has been created and tested in Argonne National Laboratory [3]. The advantages of this detector are: capability to work in cw regime, wide band of beam energies, intensities and ion types, and time resolution 20 ps. The device can be used for applications in future high-intensity machines like driver linac for the Rare Isotope Accelerator. The results of investigations of secondary electron (SE) properties and their effect on detector resolution are also presented in the paper.

2. Design features

The general layout of the BLD is shown in Fig. 1. The primary beam hits the target wire (1) and produces SE. These electrons are accelerated by a negative voltage applied to the target wire,

*Corresponding author.

E-mail address: vinogradov@phy.anl.gov
(N.E. Vinogradov).

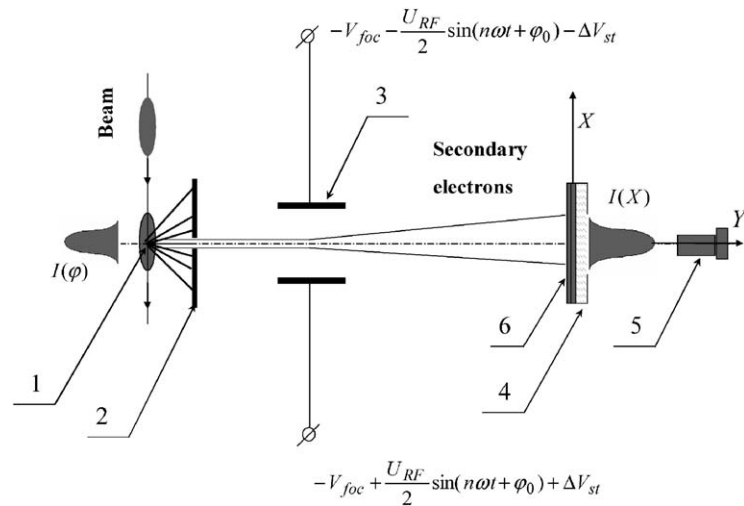


Fig. 1. General layout of the BLD: 1—tungsten target wire; 2—collimator; 3—plates of the RF deflector; 4—phosphor screen; 5—CCD camera; and 6—MCP.

collimated by the narrow slit (2) pass between RF deflector plates (3) and finally form the beam image on a phosphor screen (4). The electromagnetic field of the RF deflector is a superposition of electrostatic and RF fields. The electrostatic potential V_{foc} forms a one-dimensional focusing lens for SEs. The difference between plate voltage ΔV_{st} is used for electron beam steering. The operating frequency of the RF deflector field ω is synchronized with the fundamental accelerator frequency. Therefore, the time distribution of the bunch is coherently transformed into a spatial distribution of SEs through transverse modulation by the RF voltage. The bunch image is detected by the combination of a phosphor screen and a charge coupled device (CCD) camera (5). The multi-channel plates (MCP) (6) are used for signal amplification.

The assembly drawings of the BLD can be seen in Fig. 2. The RF deflector (2) is a quarter wave double coaxial line resonator with the electrode plates installed at the maximum RF electric field. This resonator is operated at 97 MHz and phase-locked to the accelerator master oscillator. The double coaxial line is located in air. The air–vacuum transition is achieved by a specially designed ceramic window (7) provided by Ceramaseal™ [4]. To obtain the best time resolution of

the detector, up to 30 W RF power is applied to the deflector through the water-cooled central conductors. The de-ionized water feeds the rods through cooling system connectors (6). The focusing potential V_{foc} and steering voltage ΔV_{st} are applied to the deflector electrodes through the high-voltage SHV connectors (8).

The detection of the SE beam is accomplished with the combination of a phosphor screen and light-sensitive detector. The light signal is detected by a monochromatic CCD. A dual MCP detection system is used to obtain a high gain. The second MCP lies 0.5 mm behind the first, such that the channel holes align. Both MCP are identical at 41 mm in diameter and can sustain a maximum bias of 1000 VDC each. A resistive circuit is constructed to allow both MCPs to have equal biases and run from a single power supply. The dual MCP system has a combined maximum gain of 4×10^7 . A type ^{20}P phosphor plate is situated about 0.5 mm behind the second MCP. It is biased at 3 kV relative to the MCP output to convert the accelerated electrons energy into photons of predominantly 560 nm wavelength. The quantum efficiency is estimated to be about 0.063 photons/eV/electron in this wavelength region. The electronics within the camera allow the CCD sensors to be read out in the RS-170 rastering images

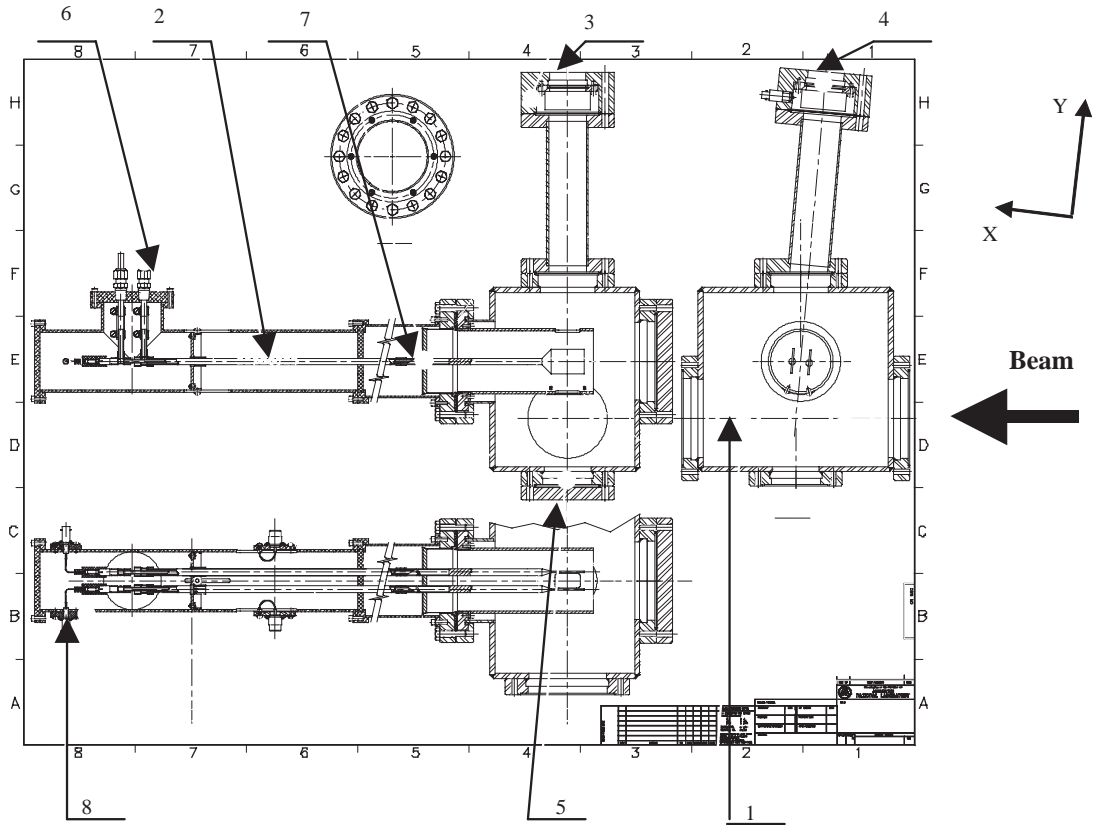


Fig. 2. Assembly drawing of the BLD: 1—main vacuum chamber; 2—RF deflector; 3—SEs beam detector based on MCP (4); 5—port for the target wire assembly; 6—water cooling connectors; 7—ceramic window; and 8—HV connectors. The coordinate system and the direction of ion beam propagation are shown for the right-side view of the drawings.

standard. The signal is amplified and then fed into a PCI-1408 frame grabber circuit board. The board features its own amplification with programmable gain to process the signal before it is delivered to an 8-bit flash ADC. This ADC is capable of sampling at up to 16.5 MHz, but operates at 12.3 MHz in the RS-170 raster mode. The image can be digitally processed in real time with the use of National Instruments [5] IMAQ software and may be restored for later reference or processing. The image signal may also be split to be monitored simultaneously with a TV monitor.

This type of registration device has several advantages including wide dynamic range and on-line observation of the bunch time profile. The

bunch center fluctuations in time, or with respect to the reference RF phase can be observed on-line.

The preliminary experiments have shown that a background signal due to parasitic low-energy SEs can appear. A 90% transmission grid under negative adjustable potential was installed upstream from the MCP to repel these electrons. The MCP and phosphor screen assembly with the grid was obtained commercially from COLUTRON [6].

The BLD target is a tungsten wire with a diameter of 0.17 mm. The target is installed on a specially constructed U-shaped spring holder that keeps the wire straight under heating. The holder is connected to a linear motion actuator that is moved by a stepper motor. This actuator is

inserted inside the beam line through a port in the BLD vacuum chamber (position 5 on Fig. 2). The stepper motor is operated from a PC that has a motor control board and an encoder reference input.

The BLD control system is constructed from the commercial product LabVIEW™. The LabVIEW™ system controls the high-voltage and RF power supplies, stepper motor controller and the CCD camera.

The BLD was installed in an Argonne Tandem Linear Accelerating System (ATLAS) beamline, 4.06 m downstream of the last superconductive resonator of the Booster section of the machine. The general view of the BLD is shown in Fig. 3. One can see the main body (1), the RF deflector (2) with HV and RF cables, and the target unit with stepper motor (3).

3. Time resolution of the detector

3.1. Properties of secondary electron emission

An ion beam of a few keV energy hitting a solid surface causes emission of electrons, protons and atomic species. In the BLD, only emission of SEs is utilized. There are a few types of SE [7]: the “true” SEs with energies < 10 eV; convoy electrons with velocity equal to the beam velocity that are emitted in the direction of a primary beam propagation; loss SE from ions carrying electrons emitted in backward direction; binary encounter electrons emitted with twice the ions velocity; and SE resulting from the decay of plasmons. Here we will consider only “true” SEs, because the intensity of other kinds of SE is relatively low and they do not affect BLD operation.

The total distribution of emitted electrons consists of angular, energy and incidence angular distributions. The energy distribution of SE is predominantly independent of the combination of projectile and target used. This distribution exhibits a sharp peak at 2.1 ± 0.3 eV that contains $\sim 85\%$ of the total amount of electrons [7]. The rest of the distribution is contained in a decaying exponential like curve. The angular distribution of ejected SE was found to be proportional to the

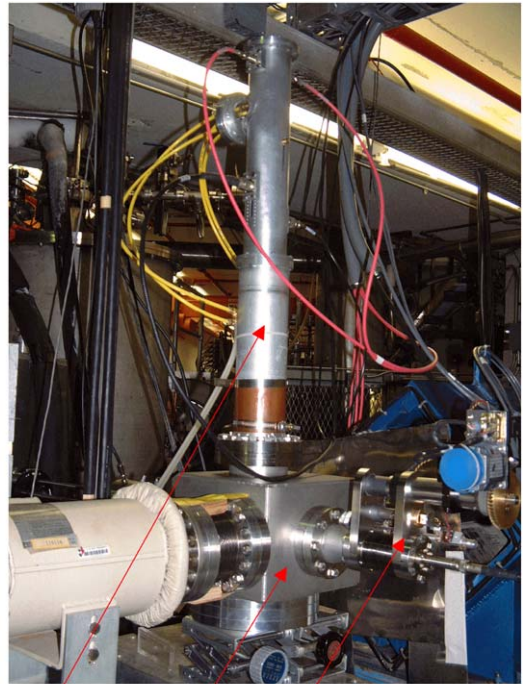


Fig. 3. General view of the BLD: 1—main vacuum chamber; 2—RF deflector; and 3—target unit with stepper motor.

cosine of the observation angle with no dependence on the angle of incidence [7]. The number of electrons produced by the interaction of a charged particle with the solid’s electrons is proportional to the electronic stopping power dE/dz of the projectile [8]. This number also increases with the incidence angle θ between oncoming ion and target surface perpendicular. Studies have shown that the incidence angular distribution of SE is proportional to $\sec \theta$ to at least 75° [9]. All these circumstances were taken into account to generate the realistic distribution of SEs for simulations.

3.2. Influence of the SE beam dynamics properties on the detector resolution

The most important characteristic of the BLD is a phase resolution [10]. The phase resolution

$\Delta\varphi = 2\pi f_0 \Delta t$ is determined by a few factors. The time Δt_{ej} necessary for the SEs to be ejected from the wire restricts the device resolution directly. It was shown [11] that the value of Δt_{ej} does not exceed 6 ps. Electrons starting from different points of the wire surface arrive at the RF deflector with a difference in time Δt_w that also perturbs the time structure of the measured bunch. The value of Δt_w can be easily estimated and is about 1 ps or less. The electron beam at the exit of collimator has the finite divergence Ψ that is defined by the size of collimator slit. Assuming the distance between the slit and the focusing plates of the deflector to be L , we can estimate the contribution of this divergence to the time resolution as $\Delta t_{dr} = \Psi^2 L / (2c\beta_e)$. For the BLD being developed, this value is about 0.3 ps. The electrostatic field of the deflector forms the focusing lens for the SE beam. The time of flight through this lens is obviously a function of distance of the electrons from the axis. It gives an additional contribution to the time resolution of the detector Δt_L . The value of Δt_L can be found from simulations because the fringing fields are important here. If the wire is not perfectly perpendicular with respect to the plane XY (see. Fig. 1) and if there is misalignment of the deflector plates, it brings an additional distortion Δt_m . The angular and energy distributions of the emitted electrons also cause the growth of the size of the output SE beam. It degrades the detector resolution by the value Δt_D that can be found from the simulations. Numerical analysis shows that the distortion of the bunch time structure due to this effect mostly happens while the SE beam moves from the wire to the collimator.

RF voltage of the deflector has major impact on the time resolution. The equation of motion along the axis X (see. Fig. 1) can be solved analytically if the electrical field between the deflector plates is supposed to be uniform and there are no fringing fields. For the particle with zero initial conditions $X(0) = 0$; $dX(0)/dt = 0$, the position of electron on the screen is

$$X = X_{\max} \sin(\varphi + \alpha) \quad (1)$$

where $\varphi = \omega t$, α is the initial phase and X_{\max} is the coordinate of the electron in the case of maximum

deflection, which is proportional to the amplitude of the electric field between the plates. A fraction of electron beam, entering the RF deflector at phase φ_0 has non-zero size Δx due to non-zero emittance of the whole SE beam. The phase resolution $\Delta\varphi_{rf}$ related to the influence of the RF deflector is determined by the value of ΔX . It can be found by differentiating of expression (1):

$$\Delta\varphi_{rf} = \frac{\Delta X}{X_{\max} \cos(\varphi_0 + \alpha)}. \quad (2)$$

Therefore, the best resolution is achieved when $\varphi_0 = -\alpha$ and $\varphi_0 = -\alpha + \pi$, and is equal to $\Delta\varphi_{rf} = \Delta X / X_{\max}$. As can be expected, the best resolution is achieved at the linear part of the sinusoidal sweeping. The value of ΔX also includes the growth of SE beam size due to initial distribution on energy and angle, and due to deflector field non-uniformity.

There are also some other effects that can influence the detector resolution. Non-linear effects due to sinusoidal sweeping of the SE beam position can worsen the resolution but it can be corrected by appropriate data analysis. The influence of space charge effects and instabilities of target, focusing and deflecting potentials are small and can be neglected. The total phase resolution of the detector can be written as

$$\Delta\varphi_{\text{tot}} = [\Delta\varphi_{aj}^2 + \Delta\varphi_w^2 + \Delta\varphi_{dr}^2 + \Delta\varphi_L^2 + \Delta\varphi_D^2 + \Delta\varphi_{rf}^2 + \Delta\varphi_m^2]^{1/2}. \quad (3)$$

The first term $\Delta\varphi_{ej}$ is a constant determined by the properties of the wire material and energy of oncoming ion beam. The next four terms can be reduced by decreasing the size of target wire, shortening the drift from the wire to the deflector and by increasing the accelerating voltage applied to wire. The term $\Delta\varphi_{rf}$ depends on two main characteristics: (1) RF voltage amplitude and (2) the width of SE beam image without RF field in the deflector. The RF voltage can be easily increased by applying higher RF power to the RF deflector and is restricted only by properties of the deflector resonator. The width of the electron beam image is defined by properties of SE and the beam optics between target wire and MCP. The conditions that allow this value to be minimized can be found from simulations.

Numerical simulation of the SE beam dynamics from the target wire under 10 kV negative potential to the location of MCP was carried out for the case when the RF voltage is turned off and on. The electrons motion in the accelerating fields from the wire to collimator slit was simulated using the FORTRAN code that was created for this purpose. The field here is calculated analytically. The SE dynamics from the slit to MCP through the electrostatic focusing field of the deflector was calculated with Simion 7 code [12]. The Simion cannot be used for simulation of all beam optics because the wire size is very small compared to the size of collimator which resulted in unacceptable calculation time and computer memory. Estimations show that the RF field phase is changed on 0.1π while the electron beam of energy about 10 keV is passing the deflector, thus the transit time factor is about $T \sim 0.98$. It allows to use quasi-electrostatic fields in these calculations. The peak RF electric field in the deflector depends on the level of applied RF power and achieves ~ 1.5 kV/cm.

The calculated electron trajectories without deflecting RF field can be seen in Fig. 4(a). The frequency count of particles at the screen location

gives the intensity distribution for the SEs beam. The size of this image limits the time resolution of the BLD. In the bunch shape measuring regime, the electron trajectories are deviated by the RF deflector. Therefore, each given phase of the primary bunch is transformed into a different position of the electron beam image. The ion bunch intensity at this phase defines the average intensity of this image. Fig. 4(b) shows an example of the deflecting influence of the RF field on the electron beam image position.

Fig. 5 shows comparison of calculated and measured shape of electron beam on the phosphor screen. The measured electron distribution is asymmetric. That is probably related to the complex interaction of primary beam hitting the edge of the target wire tangentially or can be due to some misalignments of optics elements. Since this circumstance was not considered in simulations, the calculated distribution is symmetric. The calculated width of the image as a function of electrostatic focusing voltage between the deflector plates is demonstrated in Fig. 6. It was shown that this image has a finite non-zero size for any value of focusing potential but can be minimized. Therefore, the highest resolution of the

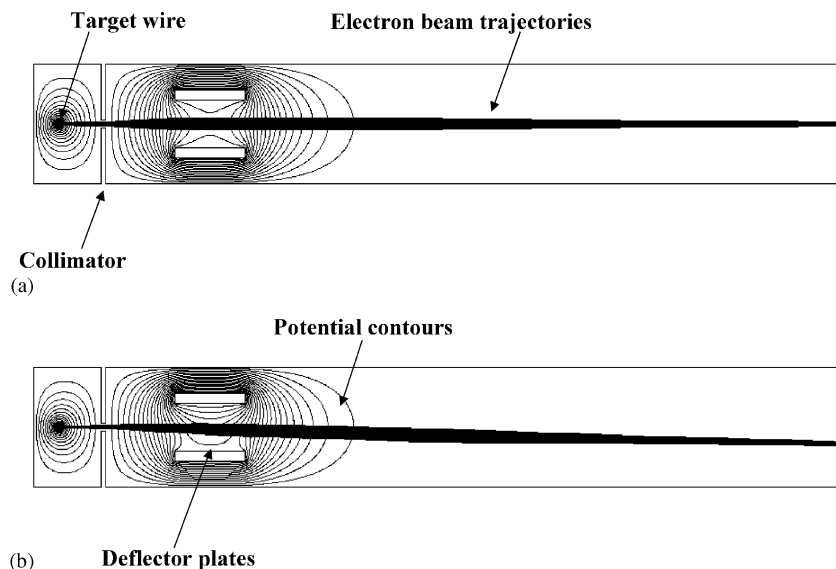


Fig. 4. Numerical simulation of the electron beam dynamics: (a) Electron trajectories without any RF power in the deflector, and (b) deflecting influence of the RF field (bunch shape measurement regime of the BLD).

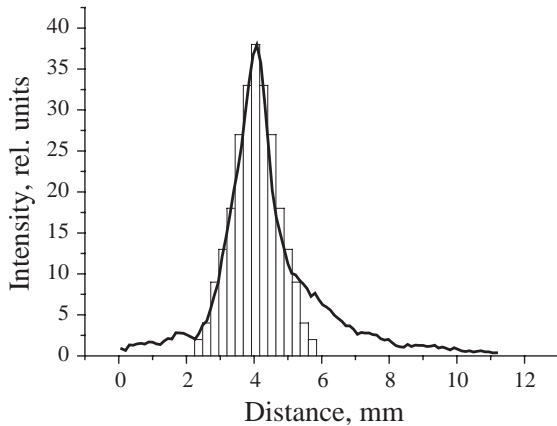


Fig. 5. Electron beam distribution on the phosphor screen. Histogram represents the simulations result and solid curve shows the measured data.

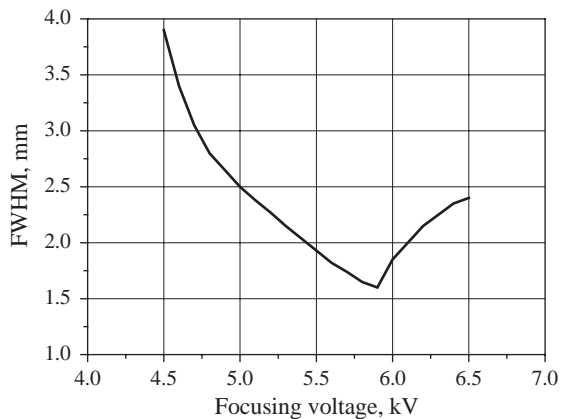


Fig. 6. FWHM of the electron beam image on the phosphor screen as a function of electrostatic focusing voltage.

BLD is achieved at $\sim 5.9 \pm 0.1$ kV focusing voltage. This result is confirmed by the experimental data.

The estimation of the total resolution of the BLD was carried out using the results of simulation and known nature of SEs emission. The contributions of terms Δt_L , Δt_D were found to be 2 and 6 ps, respectively. The beam size ΔX in Eq. (1) was about 1.6 mm and the maximum deflection X_{\max} was about 160 mm under the 30 kW RF power. Therefore, the total resolution of the BLD can be estimated as 20 ps, which correspond to 0.7° for 97 MHz frequency.

4. Beam measurements

The tests of the BLD were done at ATLAS accelerator with beams of different types. The beam energies were in the range 1.5–10 MeV/u with intensities 1–100 pA. Before a bunch shape measurement, the electron beam optics were tuned while the RF power was not applied to the RF deflector. The typical image of a well-focused electron beam is shown in Fig. 7. Here FWHM of the image size is about 1.6 mm.

4.1. Detection of energy jitter

A remarkable feature of the BLD is the possibility of on-line observation of bunch center fluctuation with respect to the reference RF phase. These fluctuations can happen due to field instabilities in the accelerator resonators. The CCD camera integrates the video signal over a 33 ms period. It means that observation of the bunch image on the TV monitor does not allow to recognize the precise value of the fluctuation frequencies. Nevertheless, the amplitude of the energy jitter can be measured successfully. To demonstrate this, a bunch center phase was measured with about a 1 s period. Since the distance between the last accelerator resonator and BLD location is known, the resolution of the energy jitter can be easily estimated from the phase jitter. Fig. 8 shows the relative energy jitter for the

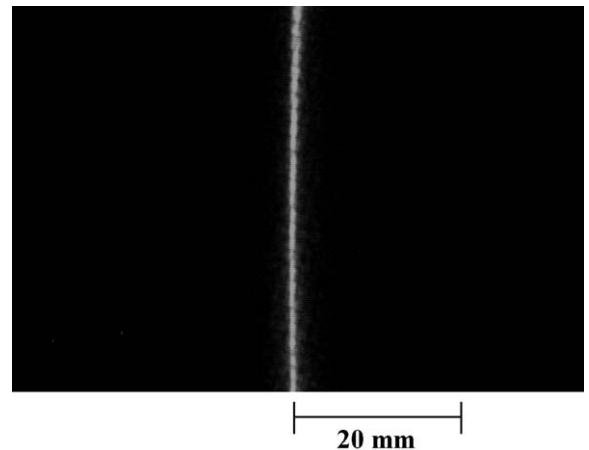


Fig. 7. Image of the focused electron beam. The scale is in mm.

153 MeV $^{16}\text{O}^{8+}$ beam. The relative resolution here is about $\sim 6 \times 10^{-4}$.

4.2. Bunch shape measurement

Fig. 9 shows the typical bunch shapes for different beams. The time resolution of these particular measurements is in the range 30–40 ps that was set in order to observe full bunch on the monitor screen. The resolution can be improved by increasing the deflecting RF voltage. For the higher RF power level, a part of the bunch distribution would be outside of the screen for the given bunch width. However, the bunch shape can be measured in this case as well. For this purpose the bunch intensity is taken with respect to some fixed reference RF phase while the whole bunch is scanned by adjusting the initial RF phase in the deflector. A fine structure of the

bunch shape in Fig. 9b) can be explained by lower value of beam current in this particular experiment.

4.3. Longitudinal emittance measurement

The BLD can also be used for the measurement of longitudinal emittance of a beam. In this experiment, several last resonators of the ATLAS Booster except the very last one were turned off. The last resonator was tuned to the regime of a bunch rotator. From the measurements of the bunch longitudinal profiles for different levels of RF field in the bunch rotator, the rms widths of the bunch were calculated. The ray-tracing code was used in order to fit the simulated bunch widths to the measured data. In this procedure the initial ellipse parameters of the beam in the longitudinal phase space are adjusted to obtain the best fitting to the measured data. This technique has been developed in INR [13]. Some results obtained using this approach are shown in Fig. 10.

4.4. The BLD as a phase detector

In this experiment, the beam energy was measured as a function of the RF field phase in the last SC resonator of the Booster. Knowing the distance between the resonator and BLD, the absolute beam energy can be observed as a function of RF phase as is seen in Fig. 11. In this case the BLD serves as a phase detector.

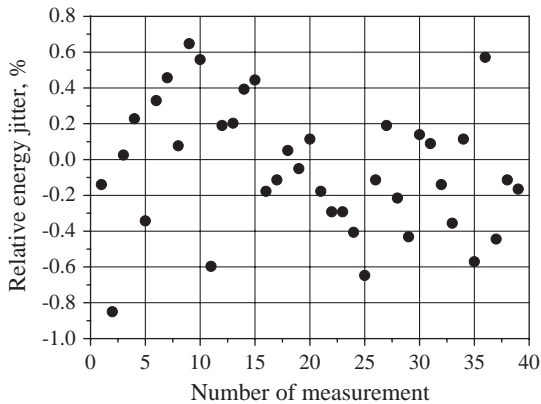


Fig. 8. Relative energy jitter $\Delta W/W$ of the bunch.

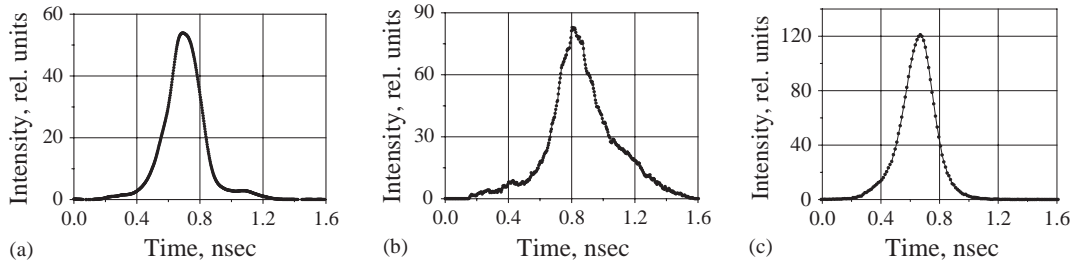


Fig. 9. Typical bunch shapes: (a) 397 MeV $^{58}\text{Ni}^{15+}$ beam, FWHM = 344 ps, (b) 153 MeV $^{16}\text{O}^{8+}$ beam, FWHM = 315 ps, and (c) 185 MeV $^{54}\text{Fe}^{16+}$ beam, FWHM = 215 ps.

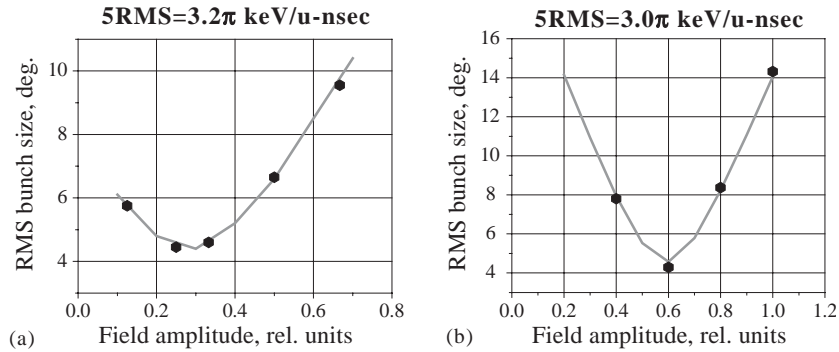


Fig. 10. Longitudinal emittance fitting. Dots are measurements, solid curves are fitted by TRACK code. (a) 85 MeV $^{20}\text{Ne}^{8+}$ beam, and (b) 185 MeV $^{54}\text{Fe}^{16+}$ beam.

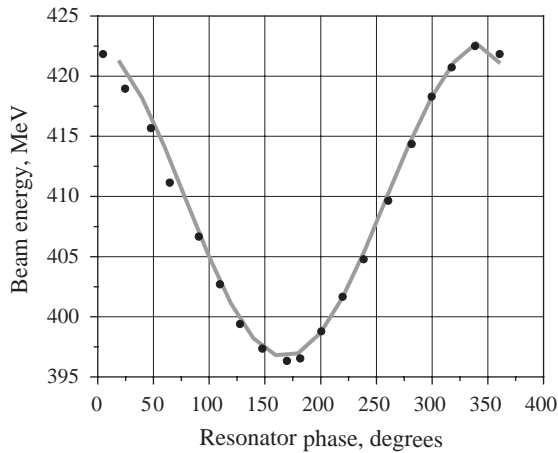


Fig. 11. Energy as a function of RF field phase in the last Booster resonator for the 397 MeV $^{58}\text{Ni}^{15+}$ beam. The solid curve represents simulation, the dots are measured data.

5. Conclusions

A new device for the measurement of bunch time profile was developed and commissioned at the ATLAS accelerator. The device is capable of measuring the bunch shape of heavy-ion beams with 20 ps resolution. The tests of BLD were done with the heavy-ion beam current as low as 1 pA and energies up to 10 MeV/u. The time resolution of the BLD was studied numerically and compared with the measured data.

References

- [1] A.V. Feshenko, Methods and instrumentation for bunch shape monitor, Proceedings of the PAC 2001, Chicago, IL, June 18–22, 2001, p. 517.
- [2] P.N. Ostroumov, Review of beam diagnostics in ion Linacs, Proceedings of the 1998 Linac Conference, Chicago, IL, August 23–28, 1998, p. 724.
- [3] N.Y. Vinogradov, et al., Bunch shape measurements of CW heavy-ion beam, Proceedings of the 2002 LINAC Conference, Gyeongju, Korea, August 19–23, 2002, p. 61.
- [4] Ceramaseal, a division of CeramTec Corporation, <http://www.ceramaseal.com/>
- [5] National Instruments Corporation, <http://www.ni.com/>
- [6] Colutron research Corporation, <http://www.colutron.com/>
- [7] H. Rothard, et al., Nucl. Instr. and Meth. B 48 (1990) 616.
- [8] A. Albert, et al., Nucl. Instr. and Meth. A 317 (1992) 397.
- [9] L.A. Diets, J.C. Sheffield, Rev. Sci. Instrum. 44 (2) (1973) 183.
- [10] A.V. Feshenko, P.N. Ostroumov, Bunch shape analyzer with transverse scanning of the low energy secondary electrons, Proceedings of the 1990 EPAC conference, Nice, France, June 12–16, 1990, p. 750.
- [11] E.S. McCrory, et al., Use of an INR-style bunch-length detector in the Fermilab Linac, Proceedings of the 1992 LINAC Conference, Ottawa, Ont., Canada, August 23–28, 1992, p. 662.
- [12] Scientific Instrument Services, Inc., <http://www.simion.com/>
- [13] Yu.V. Bylinsky, et al., Longitudinal emittance measurement of the 100 MeV proton beam, Proceedings of the PAC 1991, San Francisco, CA, May 6–9, 1991, pp. 3062–3063.